

Proceedings of the International Conference on Oxide Materials for Electronic Engineering, May 29–June 2, 2017, Lviv

Investigation of Co Ions Diffusion in Gd₃Ga₅O₁₂ Single Crystals

D. SUGAK^{a,b,*}, I.I. SYVOROTKA^{a,b}, U. YAKHNEVYCH^a, O. BURYI^a, M. VAKIV^{a,b}, S. UBIZSKII^a,
D. WŁODARCZYK^c, YA. ZHYDACHEVSKYY^{a,c}, A. PIENIAŻEK^c, R. JAKIELA^c
AND A. SUCHOCKI^{c,d}

^aLviv Polytechnic National University, Lviv, Ukraine

^bScientific Research Company “Electron–Carat”, Lviv, Ukraine

^cInstitute of Physics, Polish Academy of Sciences, Warsaw, Poland

^dInstitute of Physics, Kazimierz Wielki University, Bydgoszcz, Poland

Spatial changes of properties of Gd₃Ga₅O₁₂ (GGG) single crystals caused by diffusion of cobalt ions during high-temperature annealing (1200 °C, 24 h) in Co₃O₄ powder are investigated. The registration of these changes was carried out by optical spectrophotometry, microscopy and micro-Raman scattering methods. Changes in structure of near-surface layers of the crystal were investigated by X-ray diffraction technique. It was shown that the additional absorption induced by annealing is related to intra-center optical transitions in Co²⁺ ions, which occupy tetrahedral positions in the garnet structure at the distances of 250–500 μm from the crystal surface. The dependence of induced absorption with depth has got a non-monotonous character with a maximum at 400 μm. A comparison of the results obtained by different methods allows to suppose that the thermal treatment of GGG in the presence of cobalt ions leads to formation of the structurally and chemically non-uniform layer with a width about 500 μm.

DOI: [10.12693/APhysPolA.133.959](https://doi.org/10.12693/APhysPolA.133.959)

PACS/topics: 66.30.–h, 78.20.–e

1. Introduction

Co²⁺ doping ions occupying the tetrahedral positions in garnet lattice reveal non-linear dependence of the absorption caused by the ⁴A₂ → ⁴T₁ optical intra-center transitions. This effect, i.e. the saturation absorption of Co²⁺ ions, is used for realization of passive modulators for Q-switching of solid state lasers in 1.2–1.7 μm spectral range [1–6].

One of the most frequently used Co²⁺-doped laser materials are garnet crystals, firstly yttrium aluminum (Y₃Al₅O₁₂, YAG) and gadolinium gallium (Gd₃Ga₅O₁₂, GGG) ones [1, 4, 7–10]. In particular, both bulk GGG crystals grown by the Czochralski technique [7] and the crystalline GGG:Co²⁺ films [8–10] grown by the liquid phase epitaxy on GGG substrates are used for Q-switching.

However, cobalt ions can be present in 3+ or 2+ charge states and occupy both the tetrahedral (d) and octahedral (a) positions in garnet lattice [11]. Increase of Co²⁺(d) ions concentration is ensured by co-doping of the GGG by four-valent ions, e.g. Si⁴⁺ or Ge⁴⁺ [7–10].

At the same time, it is known that incorporation of metal ions into complex oxide crystals can be achieved by high-temperature annealing of the crystals in the metal-ions containing surroundings like metal oxides. Particu-

larly, it was shown for LiNbO₃ crystals thermally treated in powders of copper, cobalt, iron or the other metal oxides [12–14].

Purpose of this present paper is to analyze a possibility of the Co²⁺ ions incorporation into Gd₃Ga₅O₁₂ crystal by high-temperature annealing in Co₃O₄ powder as well as to study the incorporation mechanisms and depths of diffusion using optical and structural investigation methods.

2. Experimental details

The studied Gd₃Ga₅O₁₂ crystals were grown in Scientific Research Company “Electron–Carat” by the Czochralski technique from iridium crucibles in the Ar+2%O₂ atmosphere by the technology described in [15]. The samples for experiments were cut from the same bulk crystal and have got the form of (i) cylinders with a diameter of 15 mm and a height of 7 mm and (ii) plates with dimensions of 7 × 15 × 1 mm³. Both bases of cylinders and the largest edges of the plates perpendicular to [111] direction were polished.

The thermal treatment of the samples was carried out in alumina crucibles. The samples were covered by Co₃O₄ micro powder and annealed in air in a Naberterm furnace. Heating was carried out to the temperature of 1200 °C with the rate of 5 K/min. At this temperature the samples were kept for 24 h; then the samples were cooled down together with the furnace.

As is known, Co₃O₄ transforms to CoO at temperatures higher than 900 °C [16]. Therefore, annealing at

*corresponding author; e-mail: dm_sugak@yahoo.com

1200 °C occurred already in the presence of CoO only.

Optical transmission spectra of the samples were registered at room temperature in the range of 200–1700 nm by a Shimadzu UV-3600 spectrophotometer in the [111] direction, so the direction of light propagation coincided with the direction of cobalt ions diffusion. In order to study a spatial distribution of the optical absorption, i.e. its changing along the [111] direction starting from the surface that was in contact with Co_3O_4 powder, the annealed cylinder samples were cut to have the $7 \times 15 \times 2 \text{ mm}^3$ plates with the [111] direction being parallel to their largest edges.

A registration of the spatial distribution of the optical absorption was realized by special equipment, i.e. the movable table with a micrometer screw placed in the sample chamber of the spectrophotometer. The table allows to move the crystal plate relative to the specially designed immobile diaphragm. The diameter of diaphragm was equal to 100 μm . Scanning was carried out along the [111] direction, i.e. along the direction of diffusion and the light beam propagated perpendicularly to [111]. The transmission spectra were registered consequently in points with a step of 20 μm . This method was successfully used for determination of spatial distribution of coloration of lithium niobate crystals induced by reduction treatment [17–19].

Better identification of changes of the optical absorption was ensured by plotting of differential spectra obtained as a difference between the absorption in each scanned point and the absorption in the central point of the plate.

The methods of micro-Raman scattering, electron probe microanalysis and SIMS were used for determination of the changes of structure and crystal composition in the near-surface region that was in contact with cobalt oxide during annealing.

The investigations of micro-Raman scattering were carried out on the same plate cut from cylinder sample that was used for optical measurements. The experiments were performed using a Mono Vista CRS+ confocal Raman microscope-spectrometer. The Raman scattering was excited by a 532 nm laser beam that was focused on a spot of about 1 μm in diameter on a surface that was perpendicular to (111) plane. The laser beam scanned along a line from the edge of the plate to its center, i.e. along the direction of diffusion.

The same geometry of the experiment was used in the investigations by electron probe microanalysis and SIMS techniques. The electron probe microanalysis was carried out by a Hitachi SU-70 scanning electron microscope. SIMS investigations were performed by a Cameca IMS 6F mass-spectrometer.

The structural changes in the near-surface regions of the cylindrical samples were revealed by a DRON-3M X-ray diffractometer (Russia) in the reflection mode. For comparison, we also measured the reflexes from (i) the surface of the cylindrical sample that was not annealed; (ii) the surface of the segmental cylinder (the part of the

crystal that was remained after cutting of the plate) that was in direct contact with cobalt oxide powder during annealing; and (iii) from the same surface after removal of the layer of 12 μm (by polishing).

Photos of the surfaces of the plates were obtained by a Nikon ECLIPSE LV100 POL polarization microscope in the phase contrast mode.

3. Results and discussion

Annealing in air in the presence of Co_3O_4 at 1200 °C during 24 h induces the grey-brown coloration both of the cylindrical sample and the plate of $\text{Gd}_3\text{Ga}_5\text{O}_{12}$. The coloration of the samples is maximal near the surfaces that were in direct contact with cobalt oxide whereas the central part of the samples remained transparent as it was revealed after cutting of the cylindrical sample. The transmission spectra of the uncut cylindrical and plate samples are shown in Fig. 1.

The transmission spectra of the cylindrical samples were registered before and after additional polishing (Fig. 1a). As it is seen from this figure, some increase of the transmission in visible region was achieved after polishing.

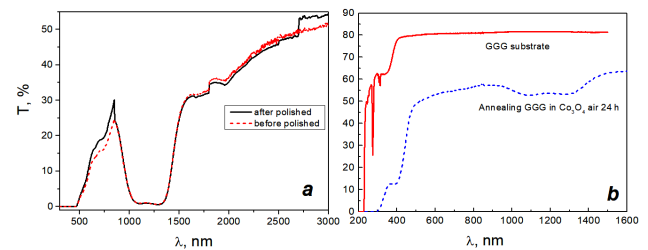


Fig. 1. Transmission spectra of $\text{Gd}_3\text{Ga}_5\text{O}_{12}$ after annealing in Co_3O_4 powder at 1200 °C — bulk (a) and plate (b) samples.

The shift of the absorption edge of $\text{Gd}_3\text{Ga}_5\text{O}_{12}$ to higher wavelengths region is taking place after annealing of the crystal (Fig. 1b). The complex absorption band in the region of 900–1600 nm is also formed.

Because the experiments on diffusion doping of GGG by heating of the crystal in the presence of cobalt oxide powder were not carried out earlier, the obtained data can be compared only with the ones obtained for crystalline materials (both bulk ones and films) doped during their growth [7–11, 20–26]. In accordance with these data the band in the region of 900–1600 nm should be related to the absorption of tetrahedrally coordinated Co^{2+} ions (${}^4A_2 \rightarrow {}^4T_1$ transition). However, the absorption caused by the ${}^5E \rightarrow {}^5T_2$ transition of tetrahedrally coordinated Co^{3+} ion can also contribute to the short-wavelength part ($\approx 1050 \text{ nm}$) of the observed band.

An investigation of the additional absorption spectra of the plate that was cut from the cylindrical sample (Fig. 2) allows to reveal the band(s) in the region of 300–800 nm.

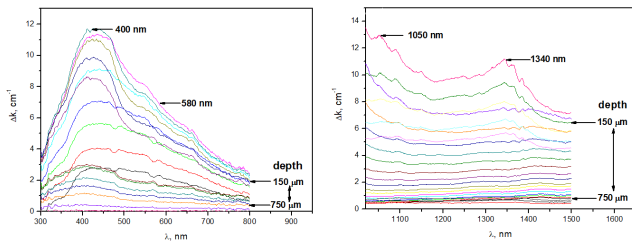


Fig. 2. Additional absorption spectra measured after annealing in the presence of Co_3O_4 at 1200°C for 24 h. The spectra were registered in the points located at different distances from the crystal edge along the direction of diffusion.

The dependence of the absorption in this region on the distance from the crystal surface is shown in Fig. 2a. Based on the results of [10, 11] one can conclude that the additional absorption in the visible region is also connected with the incorporation of cobalt ions to the crystal. It is most likely that this band is formed due to intra-center transitions in $\text{Co}^{2+}(d)$ ions (${}^4A_2 \rightarrow {}^4T_1({}^4P)$ transition) [10, 11]. The intra-center transitions of octahedrally coordinated Co^{3+} (${}^1A_1 \rightarrow {}^1T_1$) and Co^{2+} (${}^4T_1 \rightarrow {}^4A_2$) ions can also be revealed in this spectral region [10, 11]. The absorption of the complex color centers that is typical for GGG crystals doped by divalent metals [27–29] cannot be also ruled out.

In the spectral range of 1000–1500 nm the optical scanning technique allows to reveal two peaks near 1340 and 1050 nm which stand out against wide absorption band (Fig. 2b). As it is mentioned above, this peaks can be connected with ${}^4A_2 \rightarrow {}^4T_1$ transition in $\text{Co}^{2+}(d)$ ions (1340 nm) and ${}^5E \rightarrow {}^5T_2$ transition in $\text{Co}^{3+}(d)$ ions (1050 nm).

The qualitative spectra of additional absorption in 800–1000 nm spectral region were not obtained because in this region the change of the photodetectors takes place. Because of relatively low luminous flux caused by diaphragm using and high gain factors at the boundaries of the operating range of the detectors, the measurement error is essentially increased and the obtained spectral dependences of transmission are of bad quality.

As is seen from Fig. 2, the intensity of absorption essentially changes with changing of the distance from the crystal edge. A better understanding about the spatial distribution of coloration and, correspondingly, the distribution of absorbing cobalt ions can be obtained from depth dependences of absorption coefficient (Fig. 3). These dependences are registered at the wavelengths of 400, 580, 1050, and 1340 nm during scanning along the direction of diffusion from the surface of the crystal to its center. As is seen from Fig. 3, the maxima are observed at all depth dependences. The distances corresponding to these maxima from the crystal edge are about 350–450 μm .

A photograph from polarizing microscope of the surface that is perpendicular to (111) plane of the annealed

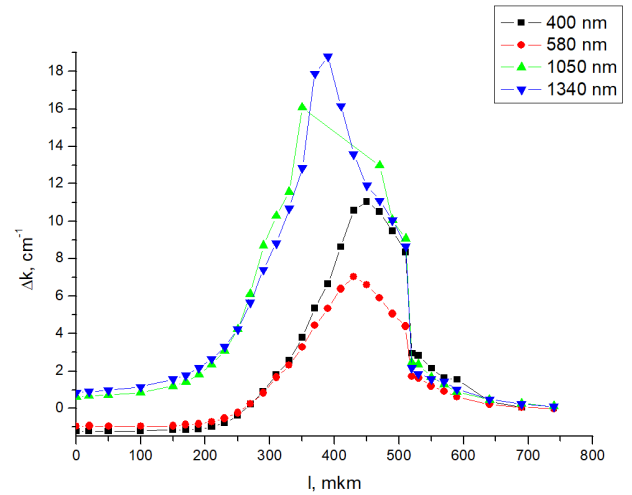


Fig. 3. The dependences of the additional absorption related to Co ions on the distance from the crystal edge.

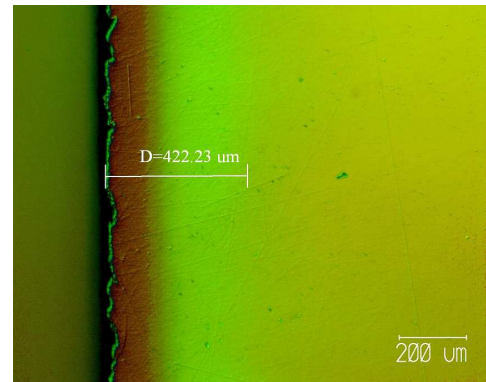


Fig. 4. A photo of diffusion region of the GGG plate after treatment.

sample is shown in Fig. 4. The thickness of the region of coloration is about 400 μm (Fig. 4) that is close to the distances where the maxima of absorption are observed (Fig. 3). The brown in color near-surface area (Fig. 4) is obviously corresponding to the region of the most intensive interaction between the environment (CoO) and the crystal.

X-ray diffraction patterns obtained from (111) planes which were in direct contact with Co_3O_4 powder during annealing as well as from the same planes of the sample that were not annealed are shown in Fig. 5. As it follows from Fig. 5a, reflexes of cobalt oxide mixture (CoO , Co_2O_3 , Co_3O_4) are clearly observed at the diffraction pattern of the annealed unpolished sample, whereas the reflex from (111) plane of GGG ($2\theta = 60^\circ$) is several times lower. After polishing (removed layer is about 12 μm), this reflex became predominant. The reflexes of cobalt oxide are also observed in this case, but their intensities are much more lower. It should be mentioned

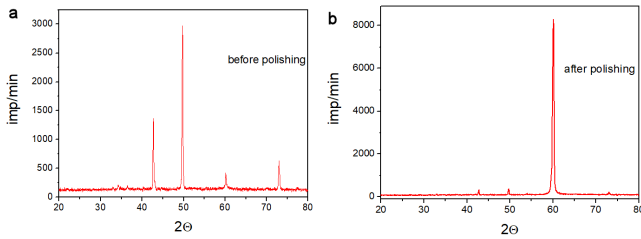


Fig. 5. Diffraction patterns of GGG surfaces just after annealing in Co_3O_4 at 1200°C (a) and after consequent polishing of sample (b).

that such polishing practically does not change the value of absorption related to Co ions, at least in the IR spectral region (see Fig. 1a).

Searching for correlation between the spatial distribution of absorption and the changes of chemical composition and structural properties caused by cobalt ions diffusion was also carried out by electron probe microanalysis, SIMS and micro-Raman scattering techniques.

The electron probe microanalysis was used for determination of the cobalt content at different distances from the edge of the plate. However, this method did not reveal a presence of cobalt in the crystal. Because the detection threshold of electron probe microanalysis is about 0.1 wt%, one has to conclude that the concentration of Co ions incorporating into the crystal is lower than this level.

More sensitive SIMS method was also used for determination of spatial distribution of cobalt concentration along the direction of diffusion. However, it was impossible to do because of high resistivity of the material (the specific resistivity of GGG is higher than $10^{14} \Omega\text{m}$ [30]).

The spectra of micro-Raman scattering obtained in the region close to the surface of annealed sample were found to be essentially different from the spectrum registered in the center of the plate. The last one is fully in line with the known data for GGG crystals [31, 32]. The differences in Raman spectra obtained at different distances from the crystal edge are illustrated by Fig. 6. As it is seen from this figure, some bands do not change their intensities with increase of the distance from the edge, whereas other ones appear and increase with increase of this distance. The positions of the maxima of all observed bands and the description of their behavior are indicated in Table I.

In order to ensure more objective comparison of the behavior of the observed bands, their intensities were related (normalized) to the intensity of the band with a maximum near 355.8 cm^{-1} which is the most intensive one in the spectrum and has got the same intensity in all points where the measurements were carried out.

The depth dependences of the relative intensity of the Raman scattering bands of the annealed GGG crystal are shown in Fig. 7. As is seen from this figure and Table I, the relative intensities of the majority of the low-energy bands ($100\text{--}700 \text{ cm}^{-1}$) are maximal near the edge of the

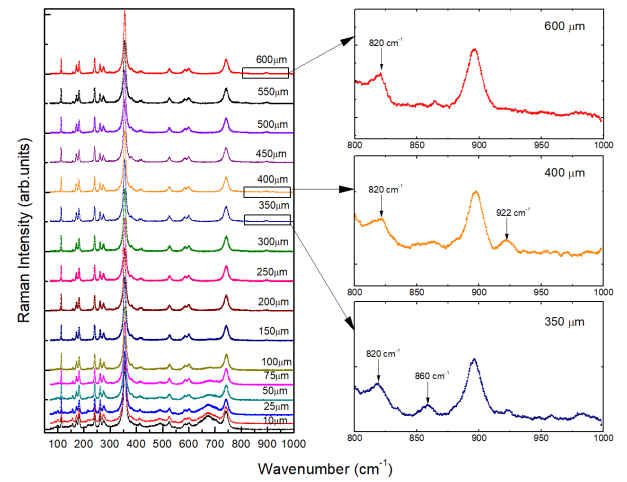


Fig. 6. The changes of Raman scattering spectra of GGG crystal with increase of the distance from the surface along the direction of cobalt ions diffusion.

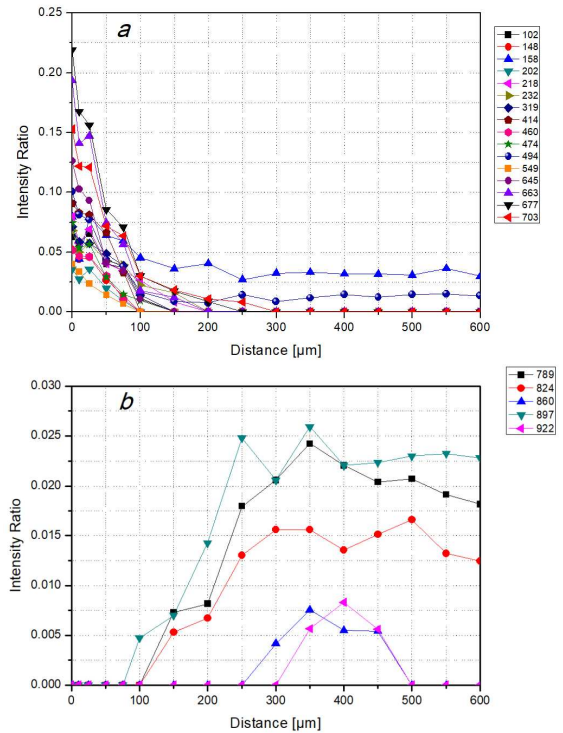


Fig. 7. The depth dependences of the relative intensity of Raman scattering bands of the annealed GGG crystal: (a) decrease of the intensity of the low-energy bands; (b) increase of the intensity of the high-energy bands.

plate and decrease to minimum at the distances about $100\text{--}200 \mu\text{m}$ (Fig. 7a). Simultaneously, increase of the high-energy bands ($789, 823.9, \text{ and } 896.6 \text{ cm}^{-1}$, Fig. 7b) begins at these distances. Their intensities saturate in direction to the center of the plate. The special subjects of interest are the Raman scattering bands with maxima

TABLE I

The spectral positions of the bands of Raman scattering in GGG crystal annealed in the presence of cobalt oxide.

Raman peak position [1/cm]	permanent	disappear at a distance about 200 μm from the crystal surface	appear at a distance of 250 μm and disappear at 500 μm
101.6		+	
113.1	+		
124.8	+		
130.5	+		
148		+	
158		+	
171.9	+		
181.8	+		
201.7		+	
217.7		+	
232.3		+	
240.9	+		
262.7	+		
275.2	+		
298.6	+		
319.4		+	
355.8	+ (main peak)		
381.4	+		
413.3	+		
414.1		+	
420.8	+		
460.4		+	
474.5		+	
493.7		+	
528.3	+		
549.3		+	
589.3	+		
601.2	+		
645.7		+	
664.3		+	
677		+	
703.2		+	
744.2	+		
789			+
823.9			+
860.2			+
896.6			+
922.4			+

near 860.2 and 922.4 cm^{-1} which appear at the distances of 250–300 μm from the edge of the plate, achieve the maxima at the distances about 400 μm and disappear (are not registered) at the ones higher than 500 μm (see Fig. 7b).

The intensive interaction of cobalt oxide with GGG crystal during thermal treatment leads to formation of the transitional layer that is structurally and chemically non-uniform. The width of this layer cannot be determined from our experiments, which is not thicker than

500 μm . The process of this layer formation is complex and cannot be described by diffusion models only, particularly, the maxima of spatial distribution cannot be predicted by such models. In the near-surface region (probably, till the depths larger than 100 μm) the structure of the transitional layer correspond not only to the garnet structure and the cobalt ions do not occupy the unambiguous positions in the garnet structure. At the distances about 250–500 μm increase and subsequent disappearing of the absorption related to Co ions occupying structural positions in the garnet lattice is observed (Fig. 3) and, simultaneously, increase and disappearing of the bands near 860.2 and 922.4 cm^{-1} in the Raman scattering spectra (Fig. 7b) is observed. So one can suppose that these peculiarities are caused by incorporation of Co ions into the regular (tetrahedral and octahedral) positions of garnet lattice. At the distances higher than 500 μm only the structure of gadolinium gallium garnet exists that reveals optical properties of the undoped GGG crystal.

4. Conclusions

The additional absorption induced by annealing is mainly caused by intra-center optical transitions in Co^{2+} ions which are incorporated into the tetrahedral positions of GGG (the bands at 300–800 nm and 900–1600 nm). Investigations of the spatial distribution of optical absorption of Co^{2+} ions show that these bands reveal themselves at the distances of 250–500 μm from the crystal surface. The dependence of induced absorption has got the non-monotonous character with a maximum near 350–450 μm from the crystal edge.

Investigations of the structure of near-surface layers of the annealed crystal by XRD technique show that the reflexes of cobalt oxide mixture are clearly observed at the diffraction pattern of the sample just after annealing, whereas the reflex from (111) plane of GGG is several times lower. However, this reflex became predominant after polishing (removed layer was about 12 μm). The reflexes of cobalt oxide are also observed in this case, but their intensities are many times lower.

The spectra of the Raman scattering are essentially different at the different distances from the crystal edge. Relative intensities of low-energy (100–700 cm^{-1}) bands decrease at the distances up to 200 μm from the crystal edge, whereas the intensities of high-energy (700–900 cm^{-1}) bands begin to increase at the distances about 100–200 μm and saturate at the distances higher than 500 μm . Generally, the Raman scattering spectra correspond to the one of undoped GGG crystal at the distances higher than 500 μm . The specific behavior is observed for Raman bands near 860.2 and 922.4 cm^{-1} : they appear at the distances about 250–300 μm from the crystal edge, achieve the maxima at 400 μm and disappear at the distances higher than 500 μm .

Obtained results allow to conclude that the thermal treatment of $\text{Gd}_3\text{Ga}_5\text{O}_{12}$ in the presence of cobalt oxide

leads to formation of structurally and chemically non-uniform layer of the width about 500 μm . At the distances from the crystal edge higher than $\sim 200 \mu\text{m}$ the cobalt ions begin to incorporate to the regular positions of the garnet lattice that is observed in absorption and Raman scattering spectra of annealed GGG crystal.

The obtained results show the possibility of formation of thin Co^{2+} doped layers of $\text{Gd}_3\text{Ga}_5\text{O}_{12}$ with a width about 200–250 μm by a diffusion during high-temperature annealing in the presence of cobalt ions.

Acknowledgments

The work was supported by the Ministry of Education and Science of Ukraine (projects DB/EMSh, 0116U004134 and DB/MEZHA, 0118U000273). The authors are grateful to Dr. Ivan Solskii (SRC “Electron-Carat”) for growth of the crystal for investigations and to Mr. Vasyly Baluk for XRD measurements. D. Włodarczyk, Ya. Zhydachevskyy, A. Pieniżek, R. Jakiela, and A. Suchocki acknowledge support of the EU within the European Regional Development Fund through the Innovative Economy grant (POIG.01.01.02-00-108/09).

References

- [1] M.B. Camargo, R.D. Stultz, M. Birnbaum, M. Kokta, *Opt. Lett.* **20**, 339 (1995).
- [2] J.B. Gruber, A. Kennedy, B. Zandi, A. Hutchinson, *Proc. SPIE* **3928**, 142 (2000).
- [3] K.V. Yumashev, I.A. Denisov, N.N. Posnov, N.V. Kuleshov, R. Moncorge, *J. Alloys Comp.* **341**, 366 (2002).
- [4] K. Kopczynski, J. Sarnecki, J. Mlynczak, Z. Mierczyk, J. Skwarcz, *Proc. SPIE* **5958**, 59582E-1 (2005).
- [5] J. Šulc, P. Arátor, H. Jelínková, K. Nejezchleb, V. Škoda, *Proc. SPIE* **6451**, 64511H-1 (2007).
- [6] H. Zhang, B. Ma, X. Chen, Q. Wang, X. Tao, P. Li, *Appl. Opt.* **52**, 8576 (2013).
- [7] V.B. Kravchenko, P.I. Sadovsii, A.T. Sobolev, L.Yu. Zakharov, S.P. Sadovsii, *Quant. Electron.* **39**, 1121 (2009).
- [8] V.V. Randoshkin, N.V. Vasil’eva, V.G. Plotnichenko, Y.N. Pyrkov, *Tech. Phys. Lett.* **26**, 1053 (2000).
- [9] V.V. Randoshkin, N.V. Vasil’eva, V.G. Plotnichenko, Y.N. Pyrkov, A.M. Saletskii, N.N. Sysoev, A.M. Galkin, V.N. Dudorov, *Phys. Solid State* **45**, 253 (2003).
- [10] K. Mazur, J. Sarnecki, J. Borysiuk, W. Wierzchowski, K. Wieteska, A. Tuross, *Thin Solid Films* **519**, 2111 (2011).
- [11] D.L. Wood, J.P. Remeika, *J. Chem. Phys.* **46**, 3595 (1967).
- [12] S. Kar, K. Bartwal, *Mater. Lett.* **62**, 3934 (2008).
- [13] U. Yakhnevych, D. Sugak, I.I. Syvorotka, O. Buryy, S. Ubizskii, in: *The Int. Research and Practice Conf. “Nanotechnology and Nanomaterials” (NANO-2017). Abstract Book*, 2017, Ed. O. Fesenko, SME Burlaka, Kiev 2017, p. 773..
- [14] D. Sugak, I. Syvorotka, O. Buryy, U. Yakhnevych, N. Martynyuk, S. Ubizskii, G. Singh, V. Janyani, H. Kumar, in: *Optical and Wireless Technologies*, Eds. V. Janyani et al., Springer Nature Singapore Pte Ltd, Singapore 2018, p. 227..
- [15] I.M. Solskii, D.Yu. Sugak, M.M. Vakiv, *Acta Phys. Pol. A* **124**, 314 (2013).
- [16] R. Ripan, I. Chetianu, *Inorganic Chemistry. Chemistry of Metals*, Mir, Moscow 1972.
- [17] D.Yu. Sugak, *Solid State Phenom.* **230**, 228 (2015).
- [18] D. Sugak, I. Syvorotka, O. Buryy, U. Yakhnevych, I. Solskii, N. Martynyuk, Yu. Suhak, G. Singh, V. Janyani, S. Ubizskii, *IOP Conf. Series Mater. Sci. Eng.* **169**, 012019 (2017).
- [19] D.Yu. Sugak, I.I. Syvorotka, O.A. Buryy, U.V. Yakhnevych, I.M. Solskii, N.V. Martynyuk, Yu. Suhak, A. Suchocki, Ya. Zhydachevskii, R. Jakiela, S.B. Ubizskii, G. Singh, V. Janyani, *Opt. Mater.* **70**, 106 (2017).
- [20] H.A. Weakliem, *J. Chem. Phys.* **36**, 2117 (1962).
- [21] H. Manaa, Y. Guyot, R. Moncorge, *Phys. Rev. B* **48**, 3633 (1993).
- [22] P.J. Dereń, W. Stręk, U. Oetliker, H.U. Güdel, *Phys. Status Solidi B* **182**, 241 (1994).
- [23] D.K. Sardar, J.B. Gruber, B. Zandi, M. Ferry, M.R. Kokta, *J. Appl. Phys.* **91**, 4846 (2002).
- [24] M.N. Taran, M. Koch-Müller, A. Feenstra, *Am. Mineral.* **94**, 1647 (2009).
- [25] M. Dondi, M. Ardit, G. Cruciani, C. Zanelli, *Am. Mineral.* **99**, 1736 (2014).
- [26] V.I. Burkov, L.N. Alyabyeva, Yu.V. Denisov, B.V. Mill’, *Inorg. Mater.* **50**, 1119 (2014).
- [27] A.O. Matkovskii, D.Yu. Sugak, S.B. Ubizskii, I.V. Kityk, *Opto-Electron. Rev.* **3**, 41 (1995).
- [28] A. Matkovskii, P. Potera, D. Sugak, L. Grigorjeva, D. Miller, V. Pankratov, A. Suchocki, *Cryst. Res. Technol.* **39**, 788 (2004).
- [29] M.A. Ellabban, M. Fally, R.A. Rupp, L. Kovacs, *Opt. Expr.* **14**, 593 (2006).
- [30] K.K. Kumar, G. Sathaiah, L. Sirdeshmukh, *Int. J. Chem. Sci.* **9**, 239 (2011).
- [31] A. Brenier, A. Suchocki, C. Pedrini, G. Boulon, C. Madej, *Phys. Rev. B* **46**, 3219 (1992).
- [32] A. Kaminska, M.G. Brik, G. Boulon, M. Karbowski, A. Suchocki, *J. Phys. Condens. Matter* **22**, 255501 (2010).